

Fabrication of Ceramic Microscale Structures

Christian[‡] and Paul J. A. Kenis[†]

Department of Chemical & Biomolecular Engineering, University of Illinois at Urbana-Champaign, Urbana, Illinois 61801

Ceramics are attractive materials for engineering applications involving high temperatures and corrosive chemicals. Here, an inexpensive and reproducible ceramic microfabrication technology was used to fabricate high-density alumina structures for applications in microchemical systems. The new method is based on the gelcasting procedure, but key drying and sintering steps have been adjusted to avoid warpage and cracking of the final structures. Centimeter-scale ceramic structures with submillimeter features can be accurately replicated from an elastomeric mold. Further study of the effect of alumina particle size, D_p , on the smallest achievable and reproducible feature size showed that excellent replication of patterns can be achieved as long as the dimensions of features in the mold are greater than $30D_p$ for the range of D_p from 0.3 to 3.0 μm .

I. Introduction

MICROCHEMICAL systems such as microcatalytic combustors, microfuel reformers, microanalytical tools, and devices for biological applications have gained considerable attention in the past few years due to their utility in portable applications and their superior performance compared with their macroscale equivalents as a result of excellent control over enhanced transport properties. Mass and heat transfer fluxes are much larger at the microscale than those at the macroscale as a result of the shorter characteristic lengths and the larger surface area-to-volume ratios.^{1–3} These favorable properties make microchemical systems suitable for various applications, including catalyst development, screening, and optimization^{4–6}; on-site synthesis of hazardous chemicals and reactive intermediates^{6–8}; and the reforming of fuels for portable power generation.^{4,9–12} Polymer-, silicon-, and metallic-based microsystems have been widely developed^{4,13–17}; however, these materials are often not suitable for reactions under harsh environments, such as high operating temperatures and corrosive reactants. Most polymers decompose around 400°C, while metals and silicon oxidize in the presence of oxygen and/or steam above 800°C and can corrode to a significant extent. Glass (e.g., quartz) is a good alternative due to its high thermal and chemical stability; however, it is not suitable for many portable applications due to its brittleness. Furthermore, machining of glass and its integration with non-glass components is difficult. Ceramics, on the other hand, have good mechanical stability in addition to their excellent thermal and chemical resistance. They are commonly used as the material of choice for gas turbines,^{18,19} engine propellers,²⁰ and insulating

devices.²¹ These same properties also render ceramics an attractive material for microscale devices involving high temperatures, corrosive reactants, and mechanically demanding environments such as microturbines,²² piezoelectric structures,^{23,24} and structures in micro-electro-mechanical-system devices.^{1,25}

To date, only a few studies have demonstrated the promise of ceramic-based microreactors for high-temperature reactions under a corrosive or oxidative environment, such as the oxidative coupling of methane at temperatures up to 1000°C.^{5,9,26,27} The reactor housings in these ceramic microreactors were fabricated using either low-pressure injection molding^{5,26} or micromachining technology,^{9,27} both of which typically involve the use of expensive equipment. Additionally, the polymer removal process in the injection molding is time consuming (i.e., ~ 7 days) due to the high polymer content in the ceramic slurry, and can cause defects such as knit lines, short shots, and thermal strains in the final ceramic structures.^{18,19,28} Costly fabrication methods, along with difficulties during the assembly and joining of different ceramic parts to obtain integrated devices, have held back the development of ceramic microchemical systems. Therefore, finding a simple, inexpensive, reliable, and reproducible ceramic microfabrication technology is crucial for the development, production, and future commercialization of ceramic microscale devices.

Gelcasting is a relatively novel, low-cost ceramic-forming method that can be used to fabricate high-quality, complex-shaped ceramic macro- and meso-scale structures.^{18,19,28–31} In this method, a concentrated slurry of ceramic powder in a solution of organic monomers is poured into a mold and polymerized *in situ* to form a solid body in the shape of the mold cavity. The low-viscosity monomer solution facilitates the transport of the ceramic slurry into the mold and the resulting polymer gel network holds the ceramic powder in the desired shape. A recently reported alternate gelcasting approach achieves polymer cross-linking via metal-ion complexation and is used in the robocasting microfabrication process.^{32–34} Gelcasting is highly preferred over the traditional ceramic-forming methods, such as slip casting and dry pressing, due to its ability to yield machinable green bodies with a high density, high strength, and low monomer content.^{35–38} Furthermore, near-net-shape, fully dense ceramic structures with excellent homogeneity can be obtained after debinding (i.e., removal of polymer) and sintering of the green bodies.^{35,36}

Gauckler and colleagues developed an alternative method, similar to gelcasting, for fabricating thin ceramic structures patterned with micrometer features by casting aqueous suspensions of ceramic powders with high solids loading onto elastomeric molds, followed by evaporation of the solvent.^{39–41} Unlike gelcasting, this method does not involve organic monomers and *in situ* polymerization. High-quality patterns with an aspect ratio of 1 and a channel width of 3 μm could be achieved using ceramic powders with an average particle size below 0.3 μm . This novel technique has been successfully used for fabricating porous ceramic microstruts in a miniaturized enzyme reactor.⁴² Some surface defects in the final sintered ceramic structures, however, were observed due to shrinkage during *in situ* drying (i.e., drying within the molds) and due to mechanical force applied during demolding of the dried thin structures. Additionally, the absence of a polymer gel network in the green bodies

J. Halloran—contributing editor

Manuscript No. 22636. Received January 5, 2007; approved May 1, 2007.

Supported by the Department of Defense Multidisciplinary University Research Initiative program administered by the Army Research Office under contract DAAD19-01-1-0582 and by the campus research board of the University of Illinois (UIUC). Christian gratefully acknowledges support of an H.G. Drickamer Fellowship from the Department of Chemical & Biomolecular Engineering at UIUC. SEM was carried out in the Center for Microanalysis of Materials, UIUC, which are partially supported by DOE grant DEFG02-91-ER45439.

[†]Author to whom correspondence should be addressed. e-mail: kenis@uiuc.edu

[‡]Christian is the full name of the first author.

reduces the green strength and green machinability. In other work, Bride *et al.*⁴³ patterned ceria-zirconia structures by impressing a plasma-etched polyimide micromold onto a soft ceramic green tape to obtain features as fine as 4 μm with an aspect ratio as high as 3. The ceramic tape was prepared using a conventional tape-casting machine, and the thickness was therefore limited to a submillimeter range.

To date, only a few studies have actually used the gelcasting method to fabricate ceramic parts for microchemical systems, such as centimeter-scale reactor housings with micrometer to submillimeter feature sizes.^{22,23,44} Liu *et al.* used gelcasting in combination with assembly mold shape deposition manufacturing (SDM) to build ceramic micro-gas turbine components with a feature size down to 200 μm .²² Also, Guo *et al.*²³ applied the gelcasting process to the fabrication of piezoelectric ceramic parts consisting of features as small as 500 μm . Other studies have noted that the reproducibility of molding and the properties of the green microstructure (e.g., density and strength) do depend on the particle size of the ceramic powder used.^{26,45} Here, we report key modifications to the gelcasting process that enable the fabrication of centimeter-scale, high-density alumina structures with micrometer to submillimeter features that are non-deformed and free of cracks. In addition, we investigate in detail the relationship between the starting alumina powder particle size and the smallest reproducible feature size in the final sintered ceramic structures and express this in a design guideline for future use.

II. Experimental Procedure

(1) Fabrication of High-Density Alumina Structures

The aqueous gelcasting forming method developed by Young *et al.* for macro- and meso-scale structures^{18,28} was adapted here to enable the fabrication of centimeter-scale, high-density, non-porous alumina structures with submillimeter features for reactor housings and lids. High-purity alumina powder (Baikalox GE1, Baikowski, Charlotte, NC) was initially deagglomerated in a high-density polyethylene bottle using a jar mill (LABMILL-8000, Advanced Ceramics Research, Tucson, AZ) containing milling media (99.9% alumina, Union Process, Akron, OH) for 48 h. The weight ratio of alumina powder to milling media was 1:3.5. The powder was then mixed with monomer solution and dispersant, and milled further using a jar mill. The monomers, here methacrylamide (98%, Aldrich, St. Louis, MO), *N,N'*-methylenebisacrylamide (99%, Aldrich), and 1-vinyl-2-pyrrolidinone (99%, Aldrich) in a 1.5:1:1.5 ratio by weight, respectively, were first dissolved in DI water to form a 20 wt% aqueous solution of monomers. The dispersant (Darvan 821A, R.T. Vanderbilt, Norwalk, CT) was then added to the mixture in the amount of 2 wt% of the total powder used. Staged addition of powder to the mixture was required to obtain a ceramic slurry with a high alumina loading, here 50 vol%, as described previously.^{35,36} The slurry was then separated from the milling media using a sieve, placed in an ice bath to prevent solvent evaporation, and de-aired in a vacuum desiccator for up to 2 h to remove any entrapped air bubbles. The de-airing step is crucial for eliminating the formation of large internal pores within the green bodies and sintered structures that can lead to cracking and low structural strength. *N,N,N',N'*-tetramethylethylenediamine (TEMED, 99%, Aldrich) and ammonium persulfate (APS, 99.99%, Aldrich) were added to the slurry (0.1 vol% of TEMED and 0.1 wt% of APS with respect to the monomer solution used) as a catalyst and an initiator, respectively, followed by stirring and de-airing in a vacuum desiccator for 30 min while the slurry was placed in an ice bath.

The alumina slurry was then poured into poly(dimethylsiloxane) (PDMS) molds carrying microchannel patterns in negative relief. These molds were obtained by replica molding of a master comprised of a positive relief structure in photoresist obtained through photolithography.¹⁴ After replica molding, the surfaces of the PDMS molds were passivated

by treatment with (tridecafluoro-1,1,2,2-tetrahydrooctyl)-1-trichlorosilane (United Chemical Technologies, Bristol, PA) for 12 h after being cleaned by a plasma sterilizer (PDC-001, Harrick, Pleasantville, NY) for about 60 s. The dimensions of the microchannels in the master were adjusted to take into account structural shrinkage during drying and thermal treatment of alumina structures so that final, high-density alumina with the desired microchannel dimensions were obtained. Catalytic polymerization of the monomers makes the alumina slurry completely solidify in the PDMS mold. The amount of catalyst and initiator was controlled so that the idle time before polymerization started was between 1 and 2 h; therefore, the slurry was sufficiently fluid during the de-airing and molding steps. In this study, the polymerization was completed approximately 3 h after the addition of the initiator. The resulting green bodies were demolded and dried in a vacuum oven (5831 E Series, Napco, Winchester, VA) at room temperature under a nitrogen atmosphere. The relative humidity inside the oven was initially maintained above 90% for 2 days, and then reduced by 10% every other day until 40% was reached. The green bodies were dried further under ambient conditions for 2 additional days. Debinding and sintering of the green bodies were performed in a high-temperature furnace (1730 HT(c), CM Furnaces, Bloomfield, NJ) in air according to an optimized thermal processing procedure (Fig. 1) to obtain crack-free and non-deformed high-density, non-porous alumina structures. The temperature was first increased to 900°C at a rate of 60°C/h and was held at 900°C for 1 h. The polymeric binder was completely removed during the initial stage of this thermal sequence, typically between 400° and 500°C.^{18,58} The temperature was further increased to 1600°C at a rate of 50°C/h for the final sintering and was held at 1600°C for 5 h. The temperature was finally reduced to 25°C at a cooling rate of 85°C/h. All SEM micrographs of the sintered alumina structures reported here were taken using a JEOL 6060-LV SEM (JEOL, Peabody, MA).

(2) Effect of Particle Size on the Smallest Reproducible Feature Size

Three high-purity $\alpha\text{-Al}_2\text{O}_3$ powders with average particle sizes of 3.0, 1.1, and 0.3 μm (Baikalox GE1, CR1, and SM8, respectively, Baikowski) were used as received. Each of these alumina powders was processed following the same procedure of deagglomeration, slurry preparation, molding, drying, debinding, and sintering as described above. In this study, the alumina loading of each ceramic slurry was fixed at 50 vol%, and identical amounts of organic monomers, DI water, dispersant, initiator, and catalyst were used. The three different ceramic slurries from alumina powders with different particle sizes were poured into PDMS molds patterned with four parallel microchannel replicas with dimensions of 150, 100, 70, and 40 μm in width and 150 μm in height. The channel width was limited to 40 μm due to the resolution of the transparency mask used dur-

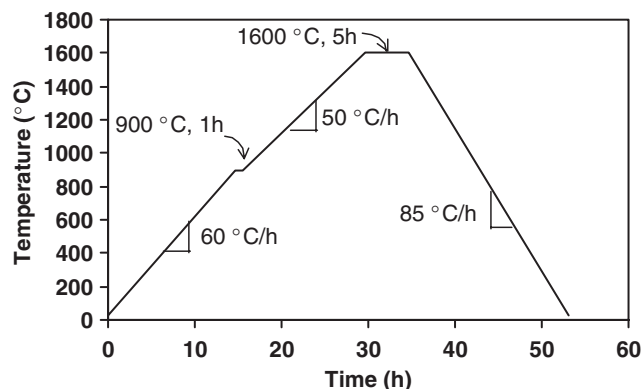


Fig. 1. Optimized thermal processing sequence for polymer removal and sintering to obtain high-density, crack-free, non-deformed alumina structures.

ing photolithography: channel replicas $<40\ \mu\text{m}$ in width were not reproducible and showed significant surface roughness, which could affect the quality of the resulting alumina structures obtained via the gelcasting method.

III. Results and Discussion

(1) Fabrication of High-Density Alumina Structures

We obtained non-deformed and crack-free centimeter-scale alumina structures with submillimeter features as shown in Fig. 2, after modification of the thermal processing steps of the original gelcasting procedure developed previously by Young *et al.* for the fabrication of ceramic structures with larger feature sizes.^{18,28} Here, we used PDMS molds with patterns of microchannel networks embossed on their surface to obtain the submillimeter features. All key modifications from the original gelcasting procedure occur after demolding of the green body.

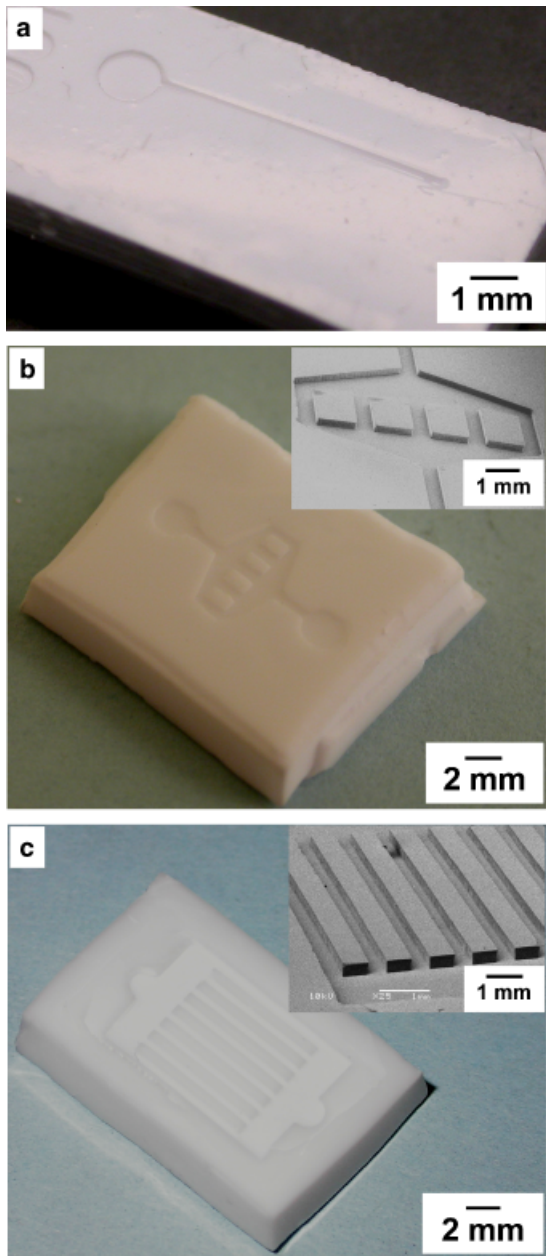


Fig. 2. Optical and scanning electron microscopy micrographs of high-density alumina structures containing microchannel slots fabricated using the modified gelcasting method: (a) one-channel design ($250\ \mu\text{m} \times 150\ \mu\text{m} \times 5\ \text{mm}$); (b) five-channel design ($400\ \mu\text{m} \times 150\ \mu\text{m} \times 1\ \text{mm}$) with 1-mm-wide walls separating the channels; (c) eight-channel design ($400\ \mu\text{m} \times 200\ \mu\text{m} \times 7\ \text{mm}$) separated by 500- μm -wide walls.

After demolding, the green bodies were dried slowly in a humidity-controlled chamber over a period of 12 days at room temperature to avoid thermal stress buildup and non-uniform shrinkage. In this optimized drying procedure, after keeping the structures at a relative humidity above 90% for 2 days, the humidity inside the chamber was reduced by $\sim 10\%$ every other day until 40% humidity was reached. Experiments with more rapid drying sequences by reducing the relative humidity, increasing the drying temperature, or a combination of both always led to cracking and deformation of the final structures. Obtaining non-deformed ceramic structures is crucial to allow for integration with each other or with other components for the actual envisioned application.

Surface spallation, implying failure in the formation of a strong binder network that results in green bodies with a powdery surface, was observed for about three in every 10 green bodies due to the inhibition of polymerization at the surface by the presence of oxygen in the PDMS molds. If necessary, this problem could be suppressed either by performing the ceramic replica molding under a nitrogen atmosphere⁴⁶ or by adding polyacrylamide to the monomer solution.⁴⁷

After completion of the drying process, the green bodies were debound (i.e., removal of the polymeric binder) and sintered according to the thermal sequence shown in Fig. 1. The heating and cooling rates of 50° to $85^\circ\text{C}/\text{h}$ used in this study were much smaller than the typical values of 100° to $300^\circ\text{C}/\text{h}$ reported in the literature for the fabrication of macro- and meso-scale ceramic structures.^{18,47,48} The higher heating and cooling rates during the polymer removal and sintering steps are not suitable for the fabrication of centimeter-scale ceramic structures. The larger surface area-to-volume ratio at the microscale leads to a more rapid heat transfer. The increase in heating rate accelerates polymeric binder decomposition and thus the rate of gas generated within the pores of the green body. This increased rate of gas generation may lead to a pressure buildup within the structure if the gas is generated faster than it can flow through the pore network and out of the ceramic body. At lower heating rates, the generated gas will have more time to escape the structure without causing deformation or cracking.

In the polymer removal and sintering steps, the dried green bodies were placed in an alumina boat within the furnace and were heated to 1600°C . During these steps, the green bodies experience structural shrinkage, resulting in thermal friction between the pieces and the boat. The surface of green bodies in contact with the alumina boat experiences a much greater resistance during shrinkage than all other surfaces due to friction. This leads to non-uniform shrinkage and structural deformation of the sintered alumina structures. In order to solve this issue, a layer of the grinding media (here, 3 mm in diameter), which was also used during the powder milling process, was poured into the alumina boat. The green bodies were then placed on top of the grinding media to avoid direct contact with the surface of the boat, and therefore the friction due to structural shrinkage can be reduced significantly and the structural deformation can be completely eliminated. The sintered alumina structures typically have densities of 95%–98% of the theoretical maximum as estimated from volume and weight measurements. The shrinkage was isotropic and averaged $13\% \pm 1\%$ linearly for structures starting from an alumina slurry with a 50 vol% solids loading. These results also indicate that, for the modified processing conditions used here, gelcasting proves to be a near-net-shape-forming technique with predictable shrinkage.

Figure 2 shows high-density alumina structures patterned with a single-channel (Fig. 2(a)), five-channel (Fig. 2(b)), and eight-channel design (Fig. 2(c)) fabricated using the gelcasting method after modification of the drying and sintering steps. High-quality replication of channels and walls, including sharp edges and corners, can be achieved with micrometer precision as evidenced by the SEM images. Prior work has typically used gelcasting to fabricate macro- and meso-scale ceramic structures consisting of parts that were as small as $\sim 500\ \mu\text{m}$. Here, we were able to produce centimeter- to millimeter-scale ceramic

structures patterned with microchannel features down to 150 μm or less (see part (2) below). We have used some of these non-deformed and crack-free alumina structures as reactor housings for high-temperature reactions under a corrosive or oxidative environment, such as the on-site production of hydrogen via the decomposition of ammonia⁴⁴ and the steam reforming of propane.⁴⁹

(2) Effect of Particle Size on the Smallest Reproducible Feature Size

Many potential applications of ceramic microscale structures require complex channel designs with submillimeter- to micrometer-sized features. To determine the smallest achievable and reproducible feature sizes for ceramic devices fabricated by the gelcasting method, we studied its dependency on the starting powder particle size in the alumina slurry. Others have observed that a reduction in the particle size of the starting powder increases the corresponding viscosity of the ceramic slurry having a high solids loading, which in turn influences the reproducibility of the ceramic structures obtained by replica molding.^{18,26,35,45} To date, however, the reproducibility of molding as a function of powder particle size has not been studied in detail.

Figure 3 shows the SEM micrographs of high-density alumina structures containing four microchannels with dimensions of approximately 130, 90, 60, and 35 μm width and 130 μm

height obtained from the replica molding of alumina slurries consisting of powders with three different average particle sizes: 3.0, 1.1, and 0.3 μm . The solids loading of the slurries was kept at 50 vol% to achieve a low linear shrinkage ($13\% \pm 1\%$) after sintering, which is an important attribute of the gelcasting method. Additionally, the amount of dispersant added to each slurry was maintained at 2 wt% of the total powder used to ensure that the viscosity of the slurries was the only variable affected by varying the particle size. Other studies typically changed the amount of dispersant added to different slurries because more dispersant is adsorbed by smaller particles due to their larger specific surface area, and thus the optimum amount of dispersant increases with decreasing particle size.^{18,45}

Consistently, we were able to obtain structures with the smallest feature sizes of approximately 90 and 35 μm when using an alumina slurry with an average particle size of 3.0 and 1.1 μm , respectively, and PDMS molds with 100 and 40 μm wide channels, respectively (Figs. 3(a) and (b)). Structures with smaller features started to exhibit flaws and significant surface roughness. Based on these results, we defined a design rule of X equals $30D_p$, where X is the smallest reproducible feature size and D_p is the average particle size of the starting alumina powder. This design rule therefore states that features in the elastomeric molds with a smallest dimension of X can be replicated as long as alumina powder with an average particle size that is 30 times smaller than X is used. The fact that we were able to obtain approximately 14 out of 15 sintered pieces from two different batches of alumina slurry for each ceramic powder illustrates the validity of the design rule as well as the reproducibility of the modified gelcasting procedure.

Next, we pushed the limits of the modified gelcasting procedure even further using alumina powder with an average particle size of 0.3 μm , for which our design rule predicts a smallest achievable feature size, X , of 10 μm . Such small dimensions, however, are beyond the maximum achievable resolution of the transparency masks used in the photolithographic fabrication of the masters. Not surprisingly, the slurry with 0.3 μm alumina powder yielded excellent replication of patterns for a 35 μm channel (Fig. 3(c)), and obtaining structures with even smaller feature sizes should still be possible, provided the desired molds are available. An earlier study by Gauckler and colleagues found that ceramic powder with an average particle size of 0.19 μm was best suited for the reproduction of thin structures patterned with ~ 5 μm features.³⁹⁻⁴¹ The result indicates that the design rule of $X \geq 30D_p$ developed in our study may also be applied to other ceramic casting methods involving suspensions with high solids loading.

IV. Conclusions

A modified gelcasting procedure for the fabrication of non-deformed and crack-free centimeter-scale alumina structures has been introduced. This optimized gelcasting method provides a simple, low-cost, reliable, and reproducible microfabrication route to obtain high-quality replication of channels and walls, including sharp edges, in alumina structures with micrometer precision. Reproducibility issues related to the use of ceramic-forming methods for the fabrication of microscale structures that, to date, have hampered the synthesis and integration of ceramic microdevices can now be avoided by using the optimized gelcasting method described herein. The production of microreactors, micro-fuel reformers, microburners, microturbines, and other mechanical tools that require small features can now be achieved inexpensively. For example, we use the high-density ceramic structures fabricated in this study as reactor housings for applications involving high temperatures and corrosive reactants, such as the decomposition of ammonia and the steam reforming of propane up to 1000°C.^{44,49}

A detailed study of the effect of alumina particle size, D_p , on the smallest achievable and reproducible feature size, X , showed that excellent replication of features with a smallest dimension

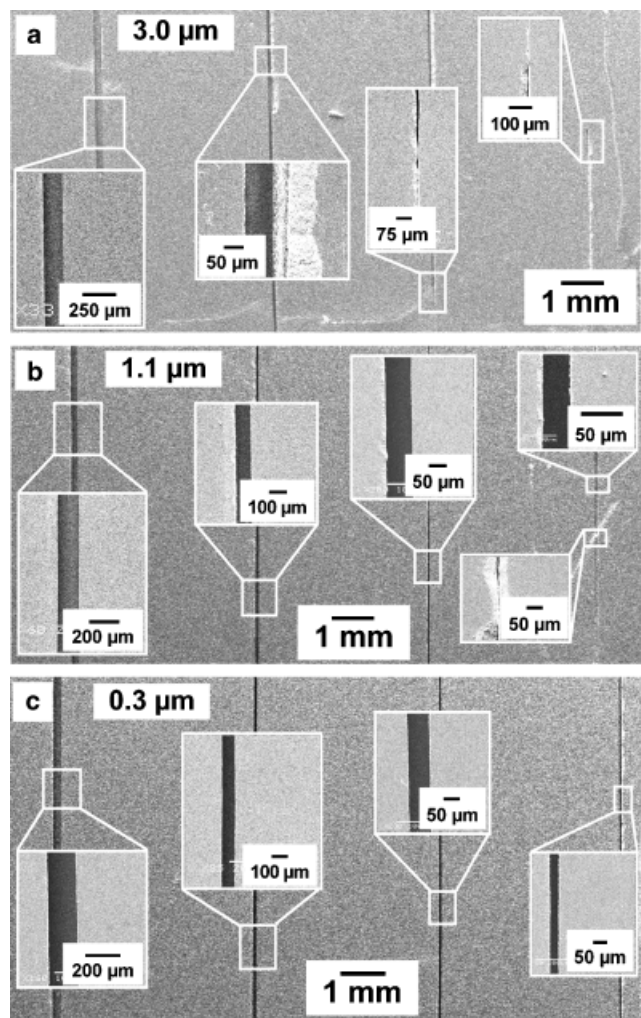


Fig. 3. Scanning electron microscopy images of sintered alumina structures patterned with four microchannel slots with dimensions of (from left to right) 130, 90, 60, and 35 μm in width and 130 μm in height, obtained using the optimized gelcasting procedure starting from ceramic slurries consisting of alumina powders with different average particle sizes of (a) 3.0 μm ; (b) 1.1 μm ; and (c) 0.3 μm .

of X can be achieved as long as alumina powder with a D_p that is 30 times smaller than X is used for the range of D_p from 0.3 to 3.0 μm . We expect that the optimized gelcasting protocols and the design rule of $X \geq 30D_p$ as reported here will aid researchers in the design and fabrication of high-quality ceramic structures with micrometer to submillimeter features.

Acknowledgment

We thank Dr. Michael Mitchell for helpful discussions.

References

- ¹K. F. Jensen, "Microchemical Systems: Status, Challenges, and Opportunities," *A.I.Ch.E.J.*, **45** [10] 2051–4 (1999).
- ²T. A. Ameel, R. O. Warrington, R. S. Wegeng, and M. K. Drost, "Miniaturization Technologies Applied to Energy Systems," *Energy Convers. Mgmt.*, **38** [10–13] 969–82 (1997).
- ³H. Löwe and W. Ehrfeld, "State-of-the-Art in Microreaction Technology: Concepts, Manufacturing and Applications," *Electrochim. Acta.*, **44** [21–22] 3679–89 (1999).
- ⁴G. Kolb, R. Zapf, V. Hessel, and H. Löwe, "Propane Steam Reforming in Micro-Channels: Results from Catalyst Screening and Optimisation," *Appl. Catal. A.*, **277** [1–2] 155–66 (2004).
- ⁵R. Knitter and M. A. Liauw, "Ceramic Microreactors for Heterogeneously Catalysed Gas-Phase Reactions," *Lab Chip*, **4** [4] 378–83 (2004).
- ⁶K. F. Jensen, "Microreaction Engineering—Is Small Better," *Chem. Eng. Sci.*, **56** [2] 293–303 (2001).
- ⁷S. K. Ajmera, M. W. Losey, K. F. Jensen, and M. A. Schmidt, "Microfabricated Packed-Bed Reactor for Phosgene Synthesis," *A.I.Ch.E.J.*, **47** [7] 1639–47 (2001).
- ⁸R. Srinivasan, I.-M. Hsing, P. E. Berger, K. F. Jensen, S. L. Firebaugh, M. A. Schmidt, M. P. Harold, J. J. Lerou, and J. F. Ryley, "Micromachined Reactors for Catalytic Partial Oxidation Reactions," *A.I.Ch.E.J.*, **43** [11] 3059–69 (1997).
- ⁹L. R. Arana, S. B. Schaevitz, A. J. Franz, M. A. Schmidt, and K. F. Jensen, "A Microfabricated Suspended-Tube Chemical Reactor for Thermally Efficient Fuel Processing," *J. Microelectromech. Systems*, **12** [5] 600–12 (2003).
- ¹⁰J. D. Holladay, E. O. Jones, M. Phelps, and J. Hu, "Microfuel Processor for Use in a Miniature Power Supply," *J. Power Sources*, **108** [1–2] 21–27 (2002).
- ¹¹J. C. Ganley, E. G. Seebauer, and R. I. Masel, "Development of a Microreactor for the Production of Hydrogen from Ammonia," *J. Power Sources*, **137** [1] 53–61 (2004).
- ¹²J. D. Holladay, Y. Wang, and E. O. Jones, "Review of Developments in Portable Hydrogen Production Using Microreactor Technology," *Chem. Rev.*, **104** [10] 4767–89 (2004).
- ¹³Y. N. Xia and G. M. Whitesides, "Soft Lithography," *Angew. Chem. Int. Ed.*, **37** [5] 551–75 (1998).
- ¹⁴D. C. Duffy, J. C. McDonald, O. J. A. Schueller, and G. M. Whitesides, "Rapid Prototyping of Microfluidic Systems in Poly(Dimethylsiloxane)," *Anal. Chem.*, **70** [23] 4974–84 (1998).
- ¹⁵A. V. Pattekar and M. V. Kothare, "A Microreactor for Hydrogen Production in Micro Fuel Cell Applications," *J. Microelectromech. Systems*, **13** [1] 7–18 (2004).
- ¹⁶Y. Kawamura, N. Ogura, T. Yamamoto, and A. Igarashi, "A Miniaturized Methanol Reformer With Si-Based Microreactor for a Small PEMFC," *Chem. Eng. Sci.*, **61** [4] 1092–101 (2006).
- ¹⁷I. Aartun, B. Silberova, H. Venik, P. Pfeifer, O. Görke, K. Schubert, and A. Holmen, "Hydrogen Production from Propane in Rh-Impregnated Metallic Microchannel Reactors and Alumina Foams," *Catal. Today*, **105** [3–4] 469–78 (2005).
- ¹⁸A. C. Young, O. O. Omatete, M. A. Janney, and P. A. Menchhofer, "Gelcasting of Alumina," *J. Am. Ceram. Soc.*, **74** [3] 612–8 (1991).
- ¹⁹O. O. Omatete, M. A. Janney, and S. D. Nunn, "Gelcasting: From Laboratory Development Toward Industrial Production," *J. Eur. Ceram. Soc.*, **17** [2–3] 407–13 (1997).
- ²⁰V. K. Pujari, D. M. Tracey, M. R. Foley, N. I. Paille, P. J. Pelletier, L. C. Sales, C. A. Willkens, and R. L. Yeckley, "Reliable Ceramics for Advanced Heat Engines," *Am. Ceram. Soc. Bull.*, **74** [4] 86–90 (1995).
- ²¹J. S. Reed, *Principles of Ceramic Processing*, 2nd edition, John Wiley & Sons, New York, 1995.
- ²²H.-C. Liu, S. Kang, F. B. Prinz, and J. Stampfl, "Fabrication of Ceramic Components for Micro Gas Turbine Engines," *Ceram. Eng. Sci. Proc.*, **23** [4] 43–48 (2002).
- ²³D. Guo, K. Cai, L. T. Li, and Z. L. Gui, "Application of Gelcasting to the Fabrication of Piezoelectric Ceramic Parts," *J. Eur. Ceram. Soc.*, **23** [7] 1131–7 (2003).
- ²⁴W. Bauer and R. Knitter, "Development of a Rapid Prototyping Process Chain for the Production of Ceramic Microcomponents," *J. Mater. Sci.*, **37** [15] 3127–40 (2002).
- ²⁵M. Heule, S. Vuillemin, and L. J. Gauckler, "Powder-Based Ceramic Meso- and Microscale Fabrication Processes," *Adv. Mater.*, **15** [15] 1237–45 (2003).
- ²⁶R. Knitter, W. Bauer, D. Göhring, and J. Haußelt, "Manufacturing of Ceramic Microcomponents by a Rapid Prototyping Process Chain," *Adv. Eng. Mater.*, **3** [1–2] 49–54 (2001).
- ²⁷R. M. Tiggelaar, J. W. Berenschot, J. H. de Boer, R. G. P. Sanders, J. G. E. Gardeniers, R. E. Oosterbroek, A. van den Berg, and M. C. Elwenspoek, "Fabrication and Characterization of High-Temperature Microreactors With Thin Film Heater and Sensor Patterns in Silicon Nitride Tubes," *Lab Chip*, **5** [3] 326–36 (2005).
- ²⁸O. O. Omatete, M. A. Janney, and R. A. Strehlow, "Gelcasting—A New Ceramic Forming Process," *Am. Ceram. Soc. Bull.*, **70** [10] 1641–9 (1991).
- ²⁹G. Tari, "Gelcasting Ceramics: A Review," *Am. Ceram. Soc. Bull.*, **82** [4] 43–7 (2003).
- ³⁰K. Prabhakaran, N. R. Babu, S. R. Kumar, and K. G. Warriar, "Freeform Gelcasting of Porous Tubular Alumina Substrate," *J. Am. Ceram. Soc.*, **85** [12] 3126–8 (2002).
- ³¹K. Cai, D. Guo, Y. Huang, and J. L. Yang, "Solid Freeform Fabrication of Alumina Ceramic Parts Through a Lost Mould Method," *J. Eur. Ceram. Soc.*, **23** [6] 921–5 (2003).
- ³²S. L. Morissette and J. A. Lewis, "Chemorheology of Aqueous-Based Alumina-Poly(Vinyl Alcohol) Gelcasting Suspensions," *J. Am. Ceram. Soc.*, **82** [3] 521–8 (1999).
- ³³S. L. Morissette, J. A. Lewis, J. Cesarano, D. B. Dimos, and T. Y. Baer, "Solid Freeform Fabrication of Aqueous Alumina-Poly(Vinyl Alcohol) Gelcasting Suspensions," *J. Am. Ceram. Soc.*, **83** [10] 2409–16 (2000).
- ³⁴M. A. Huha and J. A. Lewis, "Polymer Effects on the Chemorheological and Drying Behavior of Alumina-Poly(Vinyl Alcohol) Gelcasting Suspensions," *J. Am. Ceram. Soc.*, **83** [8] 1957–63 (2000).
- ³⁵M. A. Janney, O. O. Omatete, C. A. Walls, S. D. Nunn, R. J. Ogle, and G. Westmoreland, "Development of Low-Toxicity Gelcasting Systems," *J. Am. Ceram. Soc.*, **81** [3] 581–91 (1998).
- ³⁶M. A. Janney, S. D. Nunn, C. A. Walls, O. O. Omatete, R. B. Ogle, G. H. Kirby, and A. D. McMillan, "Gelcasting"; pp. 1–15 in *The Handbook of Ceramic Engineering*, Edited by M. N. Rahman, Marcel Dekker, New York, 1998.
- ³⁷I. Santacruz, C. Baudin, R. Moreno, and M. I. Nieto, "Improved Green Strength of Ceramics Through Aqueous Gelcasting," *Adv. Eng. Mater.*, **6** [8] 672–6 (2004).
- ³⁸K. Niihara, B. S. Kim, T. Nakayama, T. Kusunose, T. Nomoto, A. Hikasa, and T. Sekino, "Fabrication of Complex-Shaped Alumina/Nickel Nanocomposites by Gelcasting Process," *J. Eur. Ceram. Soc.*, **24** [12] 3419–25 (2004).
- ³⁹M. Heule, U. P. Schönholzer, and L. J. Gauckler, "Patterning Colloidal Suspensions by Selective Wetting of Microcontact-Printed Surfaces," *J. Eur. Ceram. Soc.*, **24** [9] 2733–9 (2004).
- ⁴⁰U. P. Schönholzer and L. J. Gauckler, "Ceramic Parts Patterned in the Micrometer Range," *Adv. Mater.*, **11** [8] 630–2 (1999).
- ⁴¹U. P. Schönholzer, N. Stutzmann, T. A. Tervoort, P. Smith, and L. J. Gauckler, "Micropatterned Ceramics by Casting into Polymer Molds," *J. Am. Ceram. Soc.*, **85** [7] 1885–7 (2002).
- ⁴²M. Heule, K. Rezwani, L. Cavalli, and L. J. Gauckler, "A Miniaturized Enzyme Reactor Based on Hierarchically Shaped Porous Ceramic Microstruts," *Adv. Mater.*, **15** [14] 1191–4 (2003).
- ⁴³J. A. Bride, S. Baskaran, N. Taylor, J. W. Halloran, W. H. Juan, S. W. Pang, and M. O'Donnell, "Photolithographic Micromolding of Ceramics Using Plasma Etched Polyimide Patterns," *Appl. Phys. Lett.*, **63** [24] 3379–81 (1993).
- ⁴⁴Christian, M. Mitchell, D.-P. Kim, and P. J. A. Kenis, "Ceramic Microreactors for On-Site Hydrogen Production," *J. Catal.*, **241** [2] 235–42 (2006).
- ⁴⁵C. G. Ha, Y. G. Jung, J. W. Kim, C. Y. Jo, and U. Paik, "Effect of Particle Size on Gelcasting Process and Green Properties in Alumina," *Mater. Sci. Eng. A*, **337** [1–2] 212–21 (2002).
- ⁴⁶J. S. Ha, "Effect of Atmosphere Type on Gelcasting Behavior of Al_2O_3 and Evaluation of Green Strength," *Ceram. Int.*, **26** [3] 251–4 (2000).
- ⁴⁷J. T. Ma, Z. P. Xie, H. Z. Miao, Y. Huang, Y. B. Cheng, and W. Y. Yang, "Gelcasting of Alumina Ceramics in the Mixed Acrylamide and Polyacrylamide Systems," *J. Eur. Ceram. Soc.*, **23** [13] 2273–9 (2003).
- ⁴⁸J. K. Montgomery, P. L. Drzal, K. R. Shull, and K. T. Faber, "Thermoreversible Gelcasting: A Novel Ceramic Processing Technique," *J. Am. Ceram. Soc.*, **85** [5] 1164–8 (2002).
- ⁴⁹Christian, M. Mitchell, and P. J. A. Kenis, "Ceramic Microreactors for On-Site Hydrogen Production from High Temperature Steam Reforming of Propane," *Lab Chip*, **6** [10] 1328–37 (2006). □